Available online at www.sciencedirect.com
ScienceDirect
Optics and Lasers in Engineering 45 (2007) 960–966
OPTICS and LASERS in ENGINEERING
www.elsevier.com/locate/optlaseng

Pulsed Nd:YAG laser welding of AISI 304 to AISI 420 stainless steels

José Roberto Berretta[a,*], Wagner de Rossi[b], Maurício David Martins das Neves[c], Ivan Alves de Almeida[b], Nilson Dias Vieira Junior[b]

[a]*Centro Tecnológico da Marinha, Av. Prof. Lineu Prestes, 2242, Cidade Universitária, 05508-900, São Paulo, Brazil*
[b]*Instituto de Pesquisas Energéticas e Nucleares, Centro de Lasers e Aplicações, São Paulo, SP, Brazil*
[c]*Instituto de Pesquisas Energéticas e Nucleares, Centro de Ciência e Tecnologia dos Materiais, São Paulo, SP, Brazil*

Received 1 November 2006; received in revised form 1 January 2007; accepted 1 February 2007
Available online 19 April 2007

Abstract

The technique to weld AISI 304 stainless steel to AISI 420 stainless steel with a pulsed Nd:YAG laser has been investigated. The main objective of this study was to determine the influence of the laser beam position, with respect to the joint, on weld characteristics. Specimens were welded with the laser beam incident on the joint and moved 0.1 and 0.2 mm on either side of the joint. The joints were examined in an optical microscope for cracks, pores and to determine the weld geometry. The microstructure of the weld and the heat affected zones were observed in a scanning electron microscope. An energy dispersive spectrometer, coupled to the scanning electron microscope, was used to determine variations in (weight %) the main chemical elements across the fillet weld. Vickers microhardness testing and tensile testing were carried out to determine the mechanical properties of the weld. The results of the various tests and examinations enabled definition of the best position for the incident laser beam with respect to the joint, for welding together the two stainless steels.

Keywords: Laser welding; Stainless steel; Welding of dissimilar materials

1. Introduction

In recent years, the consumer industry has been incorporating a variety of materials in its products made on a large scale to improve performance and reduce costs. This has resulted in increased demands for techniques to weld dissimilar materials and for use in large scale industrial production [1–3]. Among the available welding techniques, laser welding has received increasing attention [4]. One of the reasons for this is rapid development in recent years in high-energy density beam technology [5–7].

Many of the advantages and limitations of laser welding, compared to other welding processes, depend on focused beam properties. The high power density permits welding based on the keyhole principle, and the reduced energy transfer to the material produces a very narrow heat affected zone (HAZ) with low residual stress and small distortions [8]. The high cooling rate favors the formation of a fine microstructure, and this normally imparts improved mechanical properties [9,10]. On the other hand, the high cooling rates could generate the martensitic phase in the microstructure, and this phase could jeopardize some of the mechanical properties of the weld. Base material selection, component design and weld joint design are also influenced by laser welding characteristics [9].

An additional problem emerges when it involves the welding together of two materials with different metallurgical and physical properties, such as absorption at the laser wavelength, thermal conductivity and melting point. The formation of certain metallurgical phases in these materials could result in decrease in mechanical and functional properties of the joint. Decrease in solubility of alloying elements could lead to cracking. To solve these problems and to obtain welds with adequate properties it is essential to precisely control the process and the process parameters. Thus two possibilities emerge, as alternatives, to resolve this problem: modification in the temporal shape

*Corresponding author. Tel.: +55 11 38169307; fax: +55 11 38169307.
E-mail address: berretta@ipen.br (J.R. Berretta).

0143-8166/$ - see front matter © 2007 Elsevier Ltd. All rights reserved.
doi:10.1016/j.optlaseng.2007.02.001

of the pulse laser [11] or variation of the position of the laser beam with respect to the joint [12]. In the first case, it was possible to control the heating and cooling rates of the weld pool, which could improve the metallurgical characteristics of the weld region. In the second case, supply of different energies to the two materials could compensate for the differences in absorption of the laser beam and in the thermal conductivities.

Autogenously welding is the main advantage in joining dissimilar materials with a laser beam. Positioning of the focused beam by CNC facilitates location control and chemical composition of the weld fillet. This procedure requires close tolerances in the preparation of the joint. Therefore, the welding of dissimilar materials with laser beams permits high-quality joints with small HAZ to be obtained. This process can be carried out at high speeds and easily automated [13].

The main objective of this investigation was to evaluate changes in position of the incident laser beam, with respect to the joint, on the characteristics of the weld fillet, such as, its geometry, depth of penetration, formation of cracks and pores. Alloying element distribution along the cross-section of the weld and mechanical properties of the weld, determined from microhardness and tensile tests were also measured and correlated to the beam position.

2. Experimental procedure

Welding was carried out with the aid of a pulsed Nd:YAG laser, homemade, with pulse energy of up to 10 J, repetition rate of up to 500 Hz, average power of 100 W, peak power of 3 kW and pulse duration from 0.2 up to 10 ms.

The laser beam was focused at a position 3 mm below the surface of the material and the following parameters were used in the experiments: energy (E) = 6.0 J, average power (P_m) = 84 W, pulse duration (t_p) = 7 ms and pulse frequency (f) = 14 Hz. The weld fillets were prepared at a welding speed (v) = 300 mm/min and pulse overlaps of approximately 30%. Argon gas was used at a flow rate of 10 l/min.

The materials subjected to laser welding were austenitic stainless steel AISI 304 and martensitic stainless steel AISI 420. Table 1 presents the chemical compositions of the two steels, which were obtained by wave dispersive X-ray fluorescence spectroscopy.

The base materials were cut to size of 20 mm × 50 mm from 0.8 mm thick sheet. The steels were joined by autogenously welding from the top along of 50 mm.

The laser beam was positioned at the joint and moved 0.1 and 0.2 mm on either side. The specimens generated by varying the laser beam position were identified as follows: LJ—beam along the joint; MO1 and MO2—beam moved 0.1 and 0.2 mm in the direction of AISI 420 steel, respectively; A01 and A02—beam moved 0.1 and 0.2 mm in the direction of AISI 304 steel, respectively.

The joints were initially examined in an optical microscope. The cross-sections of the weld fillets were examined to determine its geometry, the depth of penetration and for cracks in the HAZ as well as the weld zone. The geometry and cross-sectional dimensions of the weld helped define its average area. With this area, and the position of the laser beam with respect to the joint, the average wt% of the main chemical elements (Cr, Ni, Fe) of the two alloys in the weld zone could be predicted.

The cross-sectional microstructures of the joints were observed in a scanning electron microscope. Energy dispersive spectroscopic measurements were carried out along the cross-section and at a depth of approximately 0.3 mm and at intervals of 0.06 mm to determine the variation, in wt%, of the main elements.

The Schaeffler diagram was used as a tool to make consistent correlations between the measured data [9]. With this diagram, the measured and estimated data were compared and the microstructure in the weld regions, obtained under the varying conditions, could be visualized. The diagram, shown later in Fig. 7, has a small triangular region in the center where ferrite and martensite are the expected microstructures. This area defines the region that renders defect-free welds.

To evaluate the mechanical properties, Vickers microhardness tests were carried out along the cross-section with a 40 g load, at a depth of 0.3 mm and at 0.07 mm intervals. This parameter was measured in the weld fillet and in the HAZ with the aid of an instrumented microhardness tester.

The tensile test was carried out to complete the evaluation and was based on the MB-4 method of ABNT (Technical Standards of the Brazilian Association). Three tensile test specimens were prepared for each type of joint. In all the tensile tests, the maximum load, the load at yield and deformation were measured. The tensile tests were carried out in a Universal testing machine with cross-head displacement rate of 5 mm/min and sampling rate of 10 points per second.

3. Results

Optical micrographs of the different weld cross-sections are shown in Figs. 1–5.

Table 1
Chemical composition of the materials

	Ni (%)	Cr (%)	Fe (%)	C (%)	Mn (%)	Si (%)	S (%)	P (%)	Mo (%)	N_2 (%)	Cu (%)
AISI 304	8.9	18.4	71.2		1.06	0.34		0.03	0.05		0.05
AISI 420	0.13	13.0	86.2		0.17	0.46		0.04			0.02

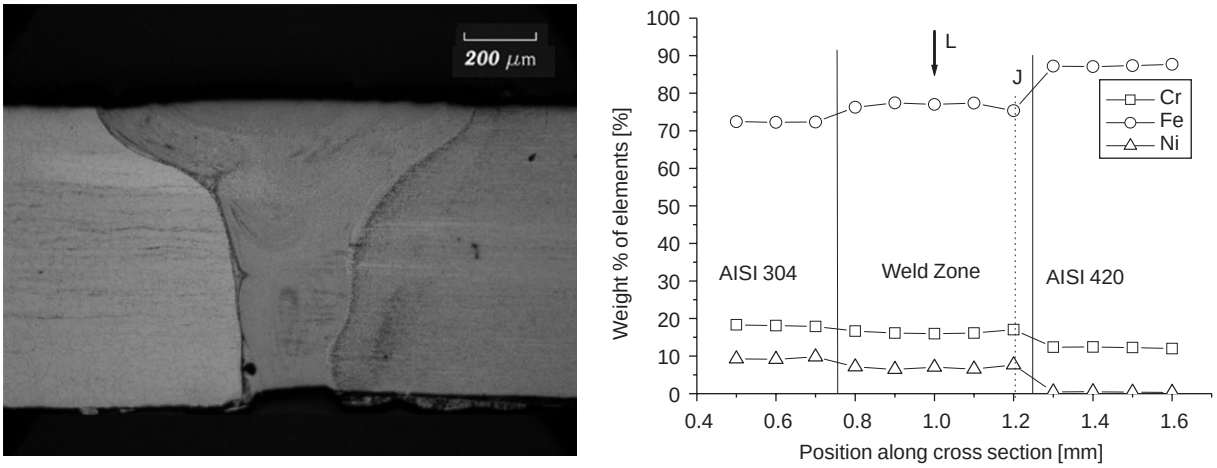

Fig. 1. Optical micrograph and graph indicating change in chemical composition along the cross-section in specimen A02, [(arrow L) laser beam (J) joint].

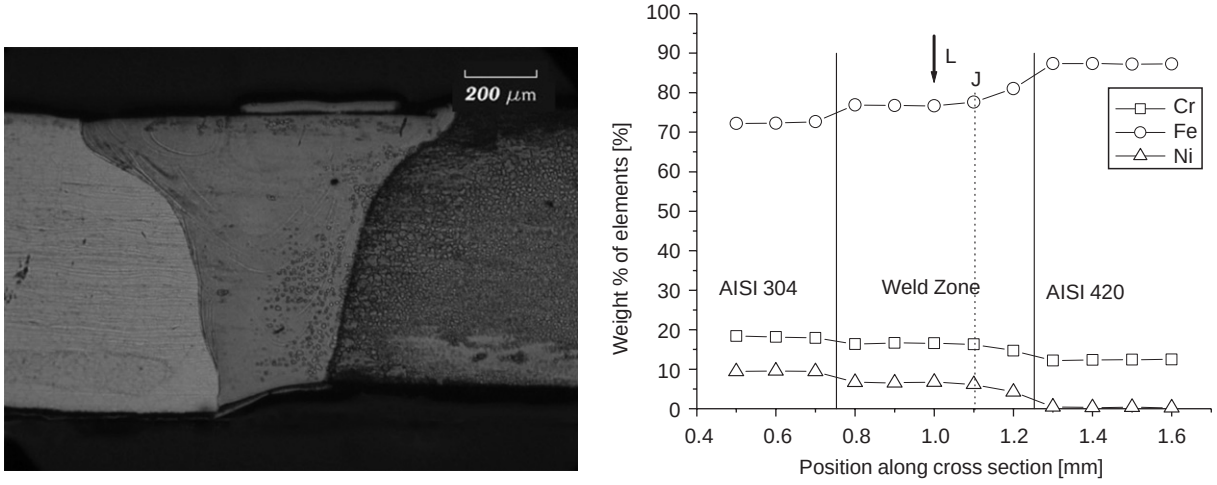

Fig. 2. Optical micrograph and graph indicating change in chemical composition along the cross-section in specimen A01 [(arrow L) laser beam (J) joint].

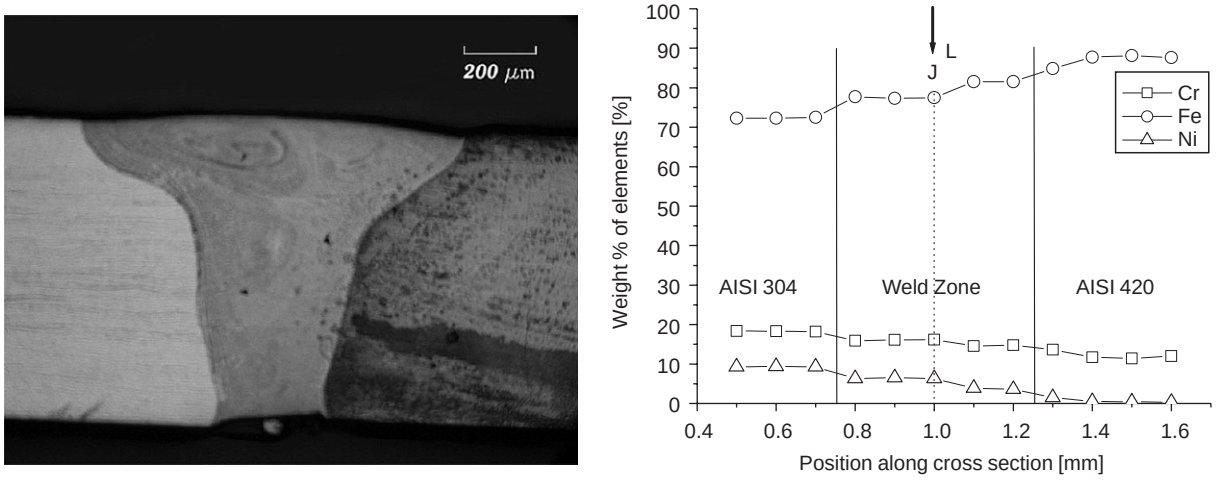

Fig. 3. Optical micrograph and graph indicating change in chemical composition along the cross-section in specimen LJ [(arrow L) laser beam (J) joint].

The specimens revealed a uniform joint, independent of the welding conditions. Variations in beam position did not affect fillet geometry, which is typical of keyhole welding.

Average width of the weld fillet was 1 mm at the surface and 0.45 mm at the root. These dimensions could adversely affect the joint between the materials if a laser beam with

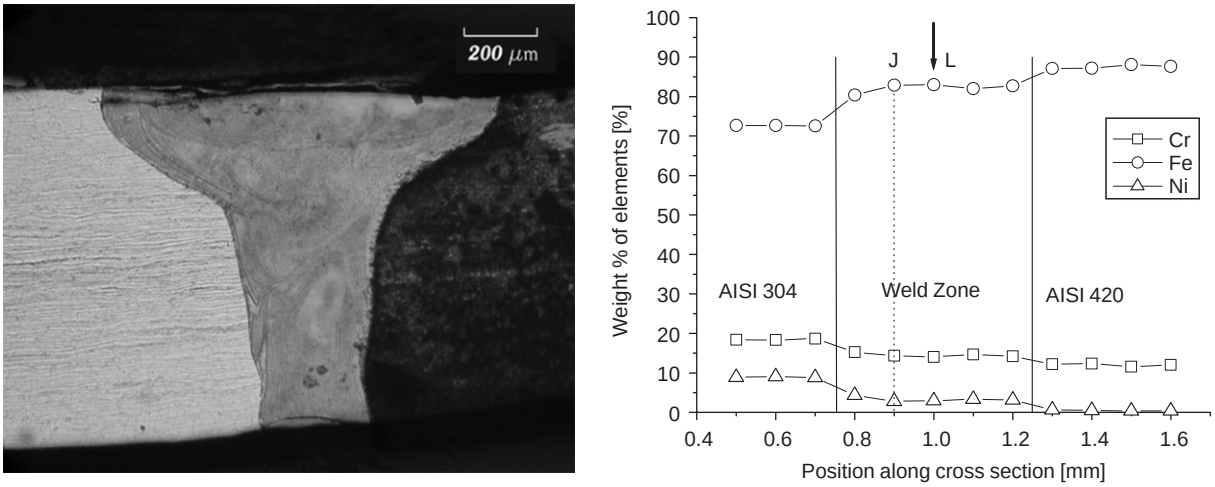

Fig. 4. Optical micrograph and graph indicating change in chemical composition along the cross-section in specimen M01 [(arrow L) laser beam (J) joint].

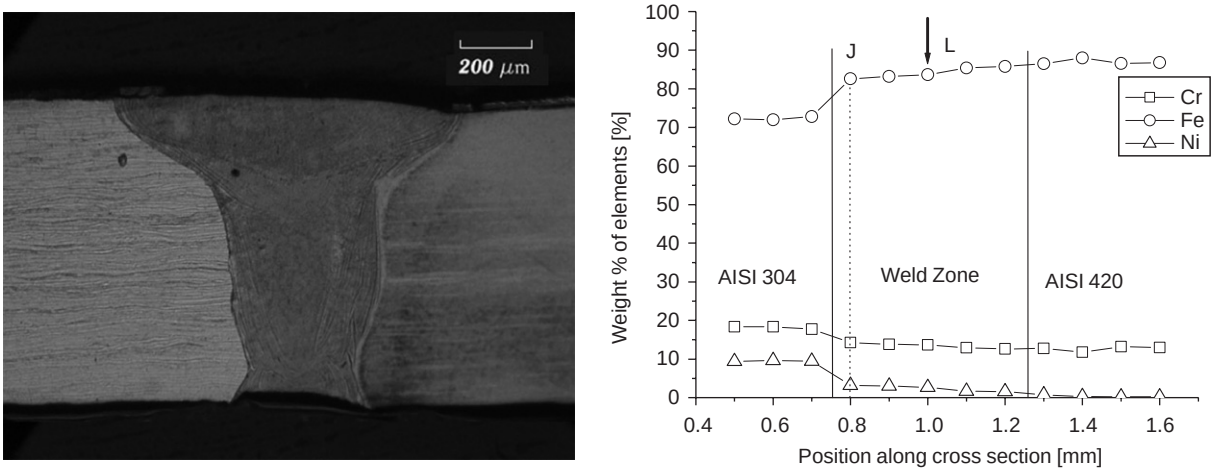

Fig. 5. Optical micrograph and graph indicating change in chemical composition along the cross-section in specimen M02 [(arrow L) laser beam (J) joint].

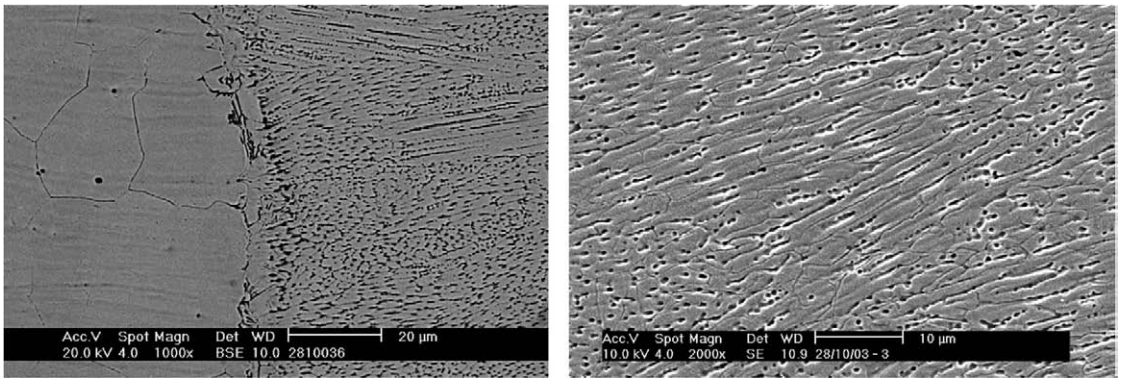

Fig. 6. Details of a typical weld zone obtained by the laser welding process, molten zone and base material (left) weld zone (right).

shifts of 0.2 mm with respect to the joint is used or by variations in the welding process.

Cracks were not observed in the weld zone and in the HAZ. Pores, formed by keyhole collapse during welding were also not observed in the cross-sections that were examined.

The graphs in Figs. 1–5 show the wt% distribution of the main elements (Cr, Ni, Fe) along the weld cross-section. It

can be observed that the elemental distribution in the weld zone is homogeneous for all laser beam positions.

The scanning electron microscopic observations revealed a fine grained microstructure, and basically dendritic in the weld zone (Fig. 6). This type of microstructure is consequent to high cooling rates, typical of the laser welding process [10].

The wt% of the main chemical elements (Cr, Ni, Fe) in the fillet cross-section were obtained by energy dispersive spectroscopy. These measurements enabled the average wt% values of the main chemical elements to be estimated. These values, shown in Table 2, suggest that the laser beam position with respect to the joint influenced the distribution of these elements, in wt%, in the weld zone.

In the Schaeffler diagram (Fig. 7) it can be seen that the estimated points formed a straight segment between the points of the base materials, foreseen in applications where the materials are dissimilar.

The Cr and Ni equivalent values are located in a region of the Schaeffler diagram with the least probability of defects in the weld fillet. It can also be seen that the welding, carried out with laser beam shifting in the direction of AISI 420 steel, facilitates the formation of a microstructure with the martensitic phase.

Table 2
EDX measured average wt% values of the main chemical elements in the laser weld fillet as a function of the beam position with respect to the joint

Specimen	Ni (wt%)	Cr (wt%)	Fe (wt%)
A02	6.95±0.45	16.18±0.44	76.67±0.88
AO1	6.07±0.29	16.12±0.18	77.80±0.41
LJ	5.33±1.46	15.53±0.78	79.13±2.22
M01	3.29±0.60	14.51±0.49	82.20±1.07
M02	2.42±0.75	13.47±0.66	84.11±1.40

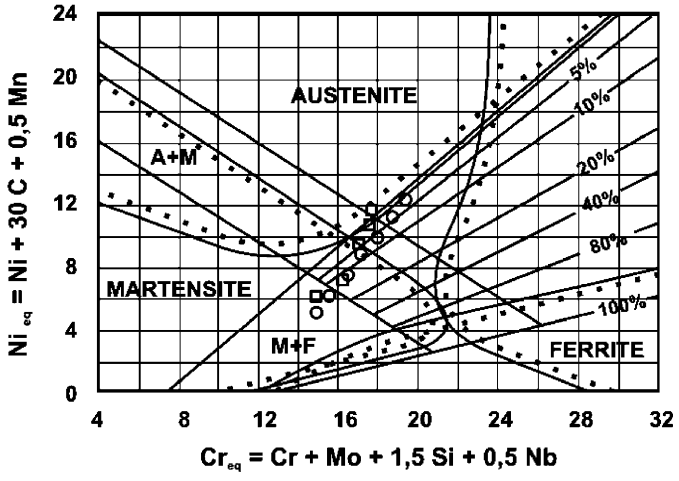

Fig. 7. Schaeffler diagram showing the average wt% points of the main chemical elements in the laser weld fillet. (circle) Foreseen and (square) measured by EDX, as a function of the beam position with respect to the joint.

Fig. 8 shows the microhardness profiles. The maximum hardness value is located in the HAZ of AISI 420 steel, and this was observed for all incident laser beam positions.

It can be seen, depending on the extent of laser beam shift from the AISI 420 steel in the direction of AISI 304 steel, that there is a gradual reduction in hardness along the cross-section of the weld zone. When the beam is shifted in the direction of AISI 420 steel, the weld zone contains a large amount of martensite, which reduces to very low values as the beam moves towards AISI 304 steel. The data obtained were in accord with the Schaeffler diagram.

Table 3 shows the tensile test results and welding efficiency. The latter is defined as the quotient between maximum load withstood by the welded material and the maximum load withstood by the base material. The maximum load of the base material was taken to be that of AISI 420 steel, as its tensile strength is lower than that of AISI 304 steel.

The efficiency of the weld can attain a maximum value of 100%. This value indicates correct adjustment of the process parameters and no material loss in autogenous laser welding. From Table 3 it can be seen that specimen LJ (with the beam on the joint) parameters furnish maximum

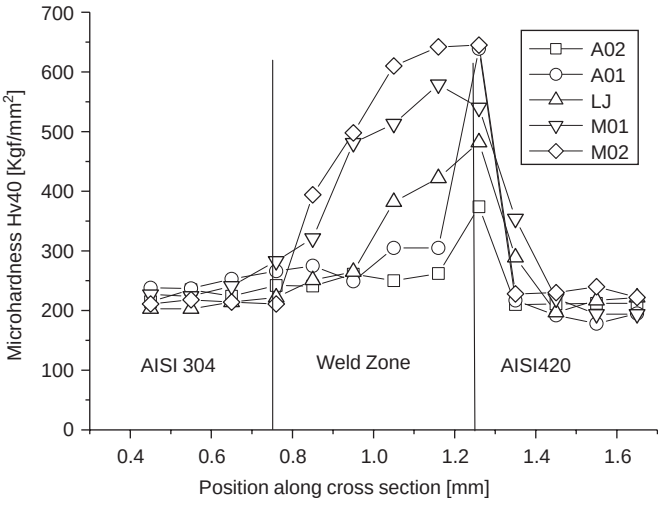

Fig. 8. Vickers microhardness profile along the cross-section of the fillet as a function of laser beam incidence with respect to the joint.

Table 3
Tensile test results

Specimen	Maximum load (kgf)	Load at yield (kgf)	Deformation (%)	Welding efficiency (%)
AISI 304	687.9±1.2	281.0±8.0	89.6±1.5	
AISI 420	679.6±2.8	428.7±11.3	24.8±0.8	
A02	152.9±4.4	—	0.59±0.07	22.5±0.6
AO1	414.8±17.1	283.4±2.2	6.3±0.9	61.0±2.5
LJ	679.5±1.9	295.3±1.6	50.5±0.3	99.9±0.1
M01	598.6±12.0	291.4±0.4	24.3±2.1	88.1±1.8
M02	326.5±12.9	285.4±0.8	2.2±0.4	48.0±1.9

welding efficiency. Fig. 9 shows specimen LJ having failed beyond the weld region.

Fig. 10 shows the surface fractured resulting from the tensile tests of the samples (A02, M02, A01 and M01). All these samples ruptured in the fillet weld. It is observed, in all of them, imperfect penetration generating areas of no welded part at the joint bottom. This fact is explained by the low energy of the pulse and the consequent small dimension of the fusion zone. Like this, when moving the laser beam in relation to joint with the overlap ratio of 30%, the welding efficiency was committed (Table 3).

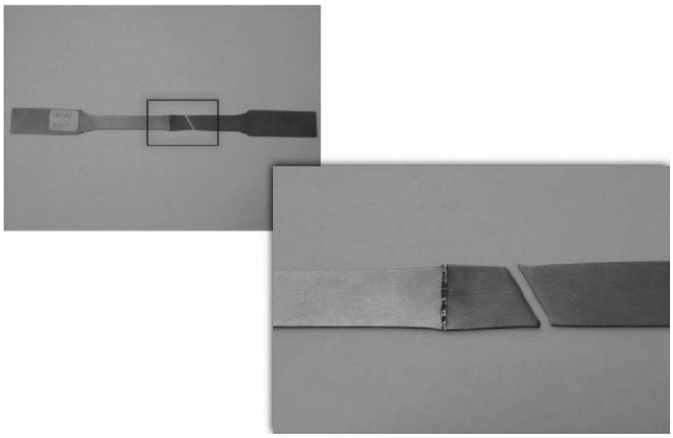

Fig. 9. Tensile test specimen LJ.

4. Conclusions

Joints obtained under all the welding conditions were uniform. Variations in beam position did not influence weld fillet geometry, which is typical of keyhole welding.

The position of the laser beam with respect to the joint influenced the wt% of the main chemical elements (Cr, Ni, Fe) in the weld zone but did not interfere with the homogeneity of the elements in the weld zone.

The weld zone revealed a fine microstructure and was basically dendritic, due to the high cooling rate, and this is characteristic of the laser welding process.

Positioning of the laser beam on the joint or its shift in the direction of AISI 304 steel favors the joint. When the laser beam is shifted in the direction of AISI 420 steel, the structure contains martensite, as foreseen.

The HAZ of AISI 420 steel, for any incident laser beam position had the highest microhardness value.

Depending on the extent of shift of the laser beam position, from the AISI 420 steel to AISI 304 steel, a gradual reduction in hardness along the cross-section of the weld zone was observed.

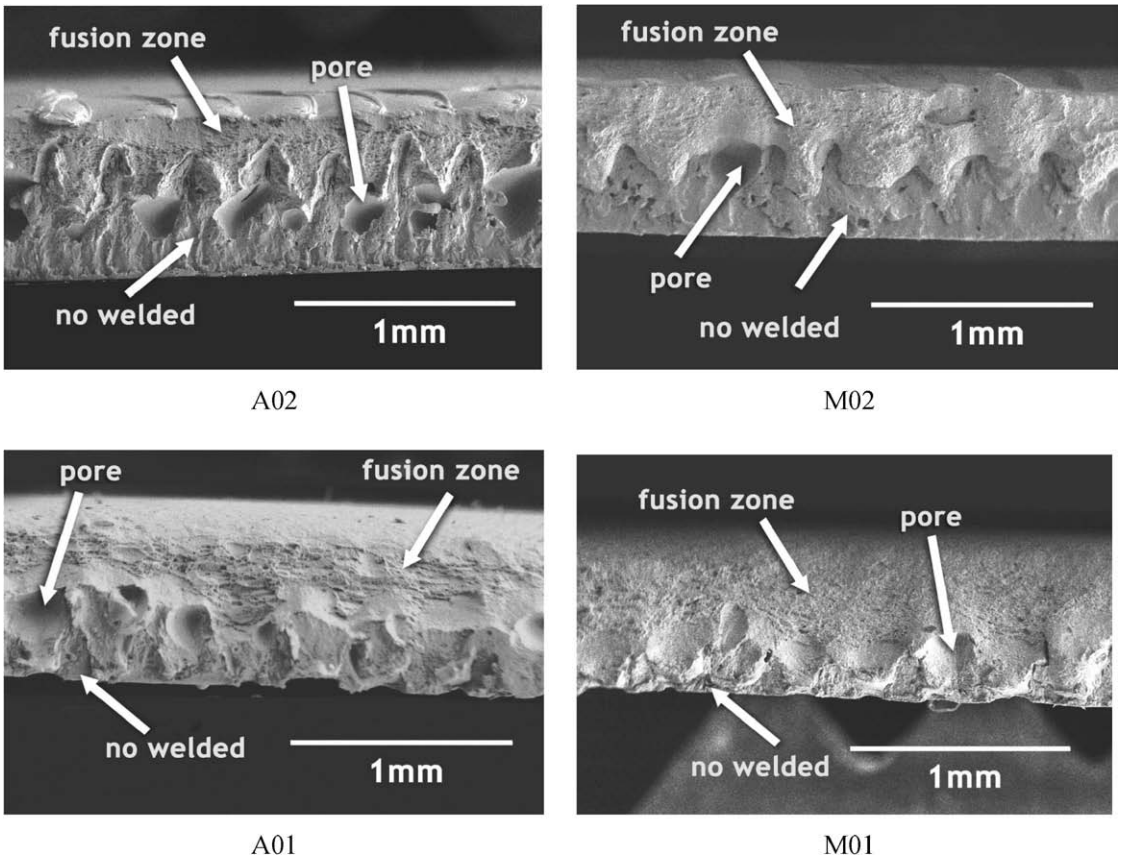

Fig. 10. Surface fractured resulting from the tensile tests of the samples (A02, M02, A01 and M01).

The specimen LJ attained the maximum welding efficiency. In the tensile test, fracture occurred outside the weld region.

The laser welding technique for dissimilar materials is a promising technique and could compete in the future with other methods that are well established and commercially used.

Acknowledgments

The authors gratefully acknowledge the financial support of CAPES and CNPq.

References

[1] Karagiannis L, Chryssolouris G. Nd:YAG laser welding—an overview. In: Third GR-I international conference on new laser technologies and applications. Proc SPIE 2003;5131:260–4.
[2] Katayama S. Laser welding of aluminium alloys and dissimilar metals. Weld Inter 2004;18(8):618–25.
[3] Zhang L, Fontana G. Autogenous laser welding of stainless steel to free-cutting steel for the manufacture of hydraulic valves. J Mater Process Technol 1998;74:174–82.
[4] Mackwood AP, Crafer RC. Thermal modeling of laser welding and related processes: a literature review. Opt Laser Technol 2005;37:99–115.
[5] Kaiser E, Schafer P. Pulse sharping optimizes the quality of seam- and spotwelds. In: Lasers in manufacturing 2005—proceeding of the third international WLT—conference on lasers in manufacturing, 2005. p. 695–8.
[6] Zhang L, Gobbi SL, Richter KH. Autogenous welding of Hastelloy X to Mar-M 247 by laser. J Mater Process Technol 1997;70: 285–92.
[7] Sun Z, Kuo M. Bridging the joint gap with wire feed laser welding. J Mater Process Technol 1999;87:213–22.
[8] Petretis Br, Balciuniene M. Peculiarities of laser welding of metals. Lithuaniam J Phys 2005;45(1):59–69.
[9] Metals Handbook, Welding, Brazing and Soldering, ASM, (9a ed.); vol. 6, 1993. ISBN 0-87170-007.
[10] Kane SF. Welding consumable development for a criogenic application. Welding Research Supplement, 1999. p. 292s–300s.
[11] Jokiel M, Durr U, Holtz R, Liebers R. Laser welding of dissimilar metals: strategies with pulsed Nd:YAG lasers. In: Lasers in manufacturing 2005—proceedings of the third international WLT-conference on lasers in manufacturing, Munich, Germany, June 2005. p. 631–6.
[12] Berretta JR, Rossi W. Laser welding of dissimilar metals with pulsed Nd:YAG laser. Doctors thesis, Instituro de Pesquisas Energéticas e Nucleares, Universidade de São Paulo, 2005.
[13] Lima MSF, Rossi W, Berretta JR. Joining titanium and steel using laser beam welding. In: 38th CIRP international seminar on manufacturing systems, 2005.